



**HAL**  
open science

## Rare-earth Metal Borosilicides $R_9Si_{15-x}B_3$ ( $R = Tb, Yb$ ): New Ordered Structures Derived from the $AlB_2$ Structure Type

Volodymyr Babizhetskyy, Volodymyr Levytskyi, Régis Jardin, Josef Bauer, Roland Guérin, Régis Gautier, Bruno Fontaine, Jean-François Halet

► **To cite this version:**

Volodymyr Babizhetskyy, Volodymyr Levytskyi, Régis Jardin, Josef Bauer, Roland Guérin, et al.. Rare-earth Metal Borosilicides  $R_9Si_{15-x}B_3$  ( $R = Tb, Yb$ ): New Ordered Structures Derived from the  $AlB_2$  Structure Type. *Journal of Inorganic and General Chemistry / Zeitschrift für anorganische und allgemeine Chemie*, 2020, 646 (14), pp.1168-1175. 10.1002/zaac.202000046 . hal-02797030

**HAL Id: hal-02797030**

**<https://univ-rennes.hal.science/hal-02797030v1>**

Submitted on 9 Jun 2020

**HAL** is a multi-disciplinary open access archive for the deposit and dissemination of scientific research documents, whether they are published or not. The documents may come from teaching and research institutions in France or abroad, or from public or private research centers.

L'archive ouverte pluridisciplinaire **HAL**, est destinée au dépôt et à la diffusion de documents scientifiques de niveau recherche, publiés ou non, émanant des établissements d'enseignement et de recherche français ou étrangers, des laboratoires publics ou privés.

# Rare-earth metal borosilicides $R_9\text{Si}_{15-x}\text{B}_3$ ( $R = \text{Tb}, \text{Yb}$ ): New ordered structures derived from the $\text{AlB}_2$ structure type

Volodymyr Babizhetskyy,<sup>\*[a]</sup> Volodymyr Levytskyy,<sup>[a]</sup> Régis Jardin,<sup>[b]</sup> Josef Bauer,<sup>[b]</sup> Roland Guérin,<sup>[b]</sup> Régis Gautier,<sup>\*[b]</sup> Bruno Fontaine,<sup>\*[b]</sup> and Jean-François Halet<sup>\*[b]</sup>

Dedicated to a long-time friend and occasional collaborator, Prof. Yuri Grin, on the occasion of his 65 Birthday.

**Abstract:** Two novel ternary borosilicides  $R_9\text{Si}_{15-x}\text{B}_3$  ( $R = \text{Tb}, x = 1.80, R = \text{Yb}, x = 1.17$ ) have been synthesized from the initial elements using tin flux method. Their crystal structures were determined by means of X-ray single crystal diffraction. Both refer to space group  $R\bar{3}2, Z = 1$ :  $a = 6.668(2) \text{ \AA}, c = 12.405(4) \text{ \AA}$  ( $R_1 = 0.027, wR_2 = 0.031$  for 1832 reflections with  $I_o > 2\sigma(I_o)$ ) for  $\text{Tb}_9\text{Si}_{15-x}\text{B}_3$ , and  $a = 6.5796(3) \text{ \AA}, c = 12.2599(5) \text{ \AA}$  ( $R_F = 0.052, wR = 0.090$  for 1369 reflections with  $I_o > 2\sigma(I_o)$ ) for  $\text{Yb}_9\text{Si}_{15-x}\text{B}_3$ . The structures represent a new structure type, derived from the  $\text{AlB}_2$ , with ordering in the metalloid sublattice resulting in distorted  $[\text{Si}_5\text{B}]$  hexagons. The presence or absence of boron in this ordered structure is discussed on the basis of difference Fourier syntheses, interatomic distances, structural analysis, and theoretical calculations in relation with the parent structures of the binaries  $\text{AlB}_2$  and  $\text{Yb}_3\text{Si}_5$  ( $\text{Th}_3\text{Pd}_5$  type of structure). Theoretical calculations show substantial covalent interactions between the metal and nonmetal elements. The small percentage of silicon atoms, which are missing in these nonstoichiometric compounds, probably allows strengthening boron-metal and boron-silicon bonding.

## Introduction

Ternary rare-earth metal boride silicide compounds are not numerous although their synthesis and investigation of their properties may constitute an interesting field for thermoelectricity application for instance.<sup>[1]</sup> Indeed, a handful of boron-rich boride silicide compounds such as  $\text{GdB}_{18}\text{Si}_5$  have been reported generally obtained by addition of small amounts of silicon to higher borides.<sup>[1]</sup> A few more have been synthesized with high silicon content.<sup>[2-8]</sup> Indeed, full investigations on phase relations in the  $R\text{-Si-B}$  systems ( $R = \text{rare-earth metal}$ ) are scarce. Ternary phase diagrams  $R\text{-Si-B}$  were reported a while ago for  $R = \text{La}, \text{Ce}, \text{Er}, \text{and Y}$  at 1070 K by Kuz'ma and colls.<sup>[9-11]</sup>

However, no evidence was given concerning the existence of ternary phases, with the exception of narrow homogeneity ranges around some binary compositions. More recently, some of us have reported the isothermal sections of some ternary systems  $R\text{-Si-B}$  ( $R = \text{Y}, \text{Nd}, \text{Gd}, \text{Dy}, \text{Ho}, \text{Er}$ ) at the temperature of 1270 K.<sup>[2-4]</sup> In general, three ternary phases were found in each system, except for Nd: The stoichiometric compound  $R_5\text{Si}_2\text{B}_8$  ( $\text{Gd}_5\text{Si}_2\text{B}_8$  structure type),<sup>[5,6]</sup> the boron-inserted Nowotny phase  $R_5\text{Si}_3\text{B}_x$  ( $\text{Mn}_5\text{Si}_3$ -type structure),<sup>[7]</sup> and the solid solution  $R\text{B}_{2-x}\text{Si}_x$  ( $\text{AlB}_2$ -type structure).<sup>[8]</sup> For the  $\text{Nd-Si-B}$  system, only  $\text{Nd}_5\text{Si}_3\text{B}_x$  was found.<sup>[3]</sup>

Over the last two decades, it has been demonstrated that metal flux is a powerful technique for the synthesis of binary or ternary compounds.<sup>[12]</sup> It provides substantial advantages for exploration of novel solid-state compounds, some of which could never be formed by conventional solid-state synthetic techniques. Indeed, numerous phases have been obtained as single crystals after removing the metallic flux matrix with moderately diluted hydrochloric acid or by electrochemical dissolving of resulted molten ingots. Using flux techniques we were ourselves able to synthesize a new series of binary silicides of formula  $R\text{Si}_{1.7}$  ( $R = \text{Dy}, \text{Ho}$ ),<sup>[13]</sup> which show ordered structures derived from the  $\text{AlB}_2$  structure type.<sup>[14]</sup> Tin as metal flux was used to obtain one of the first ternary boride silicide of the silicon-rich part of the  $R\text{-Si-B}$  phase diagram, namely  $R_8\text{Si}_{17}\text{B}_3$  ( $R = \text{Ho}, \text{Er}$ ).<sup>[8]</sup> The insertion of boron atoms within the silicon slabs in these structures generates ordered commensurate arrangements in the  $c$  direction, which are derived from the  $\text{AlB}_2$  structure type.


Using the same synthesis route, new ternary borosilicides of formula  $R_9\text{Si}_{15-x}\text{B}_3$  have been synthesized with  $R = \text{Tb}, \text{Yb}$  (see the Experimental section). Their crystal structures were solved from single-crystal X-ray diffraction data. Results indicate that they adopt a new structure type, which is derived from the  $\text{AlB}_2$  structure arrangement. Main results are reported here. The presence or absence of inserted boron in this ordered phase is discussed on the basis of difference Fourier syntheses, interatomic distances, structural analysis, and theoretical calculations in relation to the parent structures of the binaries  $\text{AlB}_2$  and  $\text{Yb}_3\text{Si}_5$  ( $\text{Th}_3\text{Pd}_5$  type of structure).<sup>[15-17]</sup>

## Results and Discussion

From preliminary X-ray studies on single crystals of  $R_9\text{Si}_{15-x}\text{B}_3$  ( $R = \text{Tb}, \text{Yb}$ ) hexagonal symmetry was found. The presence of some weak reflections leads to the consideration for tripling the  $c$  parameter of the basic unit cell. X-ray intensity data collected on an image plate or a CCD diffractometer confirm the existence of a unit cell, which can be derived from those of the  $\text{AlB}_2$  and  $\text{Th}_3\text{Pd}_5$  structure types. Tripling of the  $c$  parameter compared to

[a] Dr. V. Babizhetskyy,\* Dr. V. Levytskyy  
Department of Inorganic Chemistry  
Ivan Franko National University of Lviv  
Kyryla & Mefodiya Str. 6, UA-79005 Lviv, Ukraine  
E-mail: v.babizhetskyy@googlemail.com

[b] Dr. R. Jardin, Dr. J. Bauer,<sup>†</sup> Prof. Dr. R. Guérin, Prof. Dr. R. Gautier,  
Dr. B. Fontaine, Prof. Dr. J.-F. Halet  
Univ Rennes, Ecole Nationale Supérieure de Chimie de Rennes,  
CNRS, Institut des Sciences Chimiques de Rennes-UMR 6226  
F-35000 Rennes, France  
E-Mail: regis.gautier@enc-rennes.fr, bruno.fontaine@ensc-  
rennes.fr, halet@univ-rennes1.fr  
<sup>†</sup> Deceased 9 Aug 2016

 Supporting information for this article is available on the WWW under... or from the authors.

the unit cell of  $\text{Yb}_3\text{Si}_5$  ( $\text{Th}_3\text{Pd}_5$  type)<sup>[13, 16]</sup> was found. The collected diffraction data revealed a decrease in the unit cell parameters and volumes from Tb to Yb, thus a good agreement with the lanthanide contraction law. The Laue groups  $\bar{3}$  and  $\bar{3}m$  led to the possible space groups  $R\bar{3}$ ,  $R\bar{3}$ ,  $R32$ ,  $R3m$ , and  $R\bar{3}m$ . The best solution and the structure refinements were reached using the non-centrosymmetric space group  $R32$ . Crystal structure and refinement details are given in Table 1.

**Table 1.** Crystal data and structure refinement details for  $\text{Tb}_9\text{Si}_{15-x}\text{B}_3$  and  $\text{Yb}_9\text{Si}_{15-x}\text{B}_3$ .

Composition	$\text{Tb}_9\text{Si}_{15-x}\text{B}_3$ ( $x = 1.80$ )	$\text{Yb}_9\text{Si}_{15-x}\text{B}_3$ ( $x = 1.17$ )
Crystal system	trigonal	trigonal
Space group	$R32$ (No 155)	$R32$ (No 155)
Pearson symbol	$hR27$	$hR27$
Formula per unit cell, Z	1	1
Lattice parameters		
$a / \text{\AA}$	6.668(1)	6.5896(3)
$c / \text{\AA}$	12.404(4)	12.2599(5)
Unit cell volume / $\text{\AA}^3$	477.7(2)	459.64(4)
Calculated density / ( $\text{g/cm}^3$ )	6.373	7.146
Absorption coefficient / ( $1/\text{mm}$ )	39.911	45.23
Crystal size / $\text{mm}^3$	0.01 x 0.017 x 0.23	0.02 x 0.02 x 0.18
Radiation and wavelength / $\text{\AA}$	Mo K $\alpha$ , 0.71073	Mo K $\alpha$ , 0.71073
Diffractometer	STOE IPDS II	Nonius Kappa CCD
Refined parameters	18	18
Refinement	$F^2$	$F$
$2\theta_{\text{max}}$ and $(\sin\theta/\lambda)_{\text{max}}$	63.06, 0.736	70.0, 0.807
$h, k, l$	$-9 < h < 9$	$-10 < h < 5$
Collected reflections	$-9 < k < 9$	$0 < k < 10$
Independent reflections	$-18 < l < 15$	$0 < l < 17$
Reflections with $I_o > 2\sigma(I_o)$	1832	1369
Reflections with $I_o > 2\sigma(I_o)$	364 ( $R_{\text{int}} = 0.047$ )	438
Final $R_1^{[a]}$ indices ( $R_1^{[a]}$ all data)	0.027 (0.046)	0.053
Weighted $wR_2^{[b]}$ factor ( $wR_2^{[b]}$ all data)	0.061 (0.070) <sup>[c]</sup>	0.090 <sup>[d]</sup>
Goodness-of-fit on $F^2$ :	0.96	1.1
Flack parameter	0.07(15)	0.05(17)
Largest diff. peak and hole / ( $e/\text{\AA}^3$ )	1.41/-1.01	2.39/-2.36

<sup>[a]</sup>  $R_1(F) = [\sum(|F_o| - |F_c|)] / \sum|F_o|$ . <sup>[b]</sup>  $wR_2(F^2) = [\sum[w(F_o^2 - F_c^2)^2] / \sum[w(F_o^2)^2]]^{1/2}$ .

<sup>[c]</sup>  $[w^{-1} = \sigma^2(F_o)^2 + (0.0122P)^2 + 0.000P]$ , where  $P = (F_o^2 + 2F_c^2) / 3$ .

<sup>[d]</sup>  $R_w$ , where  $w = 1 / (\sigma^2(F_o)^2 + (0.0056F_o^2)^2)$ .

The atomic coordinates and isotropic displacement parameters are listed in Table 2 whereas the anisotropic displacement parameters are given in Table 3. In the crystal structure of these compounds, the rare-earth metal atoms occupy the special  $9d$  Wyckoff positions. For the ordered metalloid sublattice, three positions were found:  $9e$  (Si1) and  $6c$  (Si2) for silicon atoms and  $3b$  for boron atoms. In order to locate the boron atoms, difference Fourier maps have been established and a residual electronic density peak in the  $3b$  site of the trigonal unit cell was revealed. The attribution of this peak to boron led to the decreasing of the weighted reliability factor  $R_w$  from 0.070 to 0.061. The final difference Fourier analyses gave no indications for additional atomic sites. The isotropic displacement parameters for Si1 atoms located in the  $9e$  site in both refinements for  $\text{Tb}_9\text{Si}_{15}\text{B}_3$  and  $\text{Yb}_9\text{Si}_{15}\text{B}_3$  crystal structures showed rather large values. We therefore refined the occupation factor for Si1 ( $\text{SOF} = 0.80(2)$  and  $\text{SOF} = 0.87(4)$  for  $\text{Tb}_9\text{Si}_{15}\text{B}_3$

and  $\text{Yb}_9\text{Si}_{15}\text{B}_3$ , respectively). Final difference Fourier synthesis did not mention any significant residual electronic density peaks (Table 1). The final formula of these boride silicides deduced from the structure refinements, are  $\text{Tb}_9\text{Si}_{15-x}\text{B}_3$  ( $x = 1.80$ ) and  $\text{Yb}_9\text{Si}_{15-x}\text{B}_3$  ( $x = 1.17$ ), respectively. The corresponding ratios Tb/Si = 40.54/59.46 and Yb/Si = 39.42/60.58 agree well with the nominal composition obtained by EDS measurements: R/Si = 40.06/59.94 (see the Experimental section). Observed and calculated structure factors can be obtained from the authors on request.

**Table 2.** Atomic coordinates and isotropic displacement parameters (in  $\text{\AA}^2$ ) for  $\text{Tb}_9\text{Si}_{15-x}\text{B}_3$  and  $\text{Yb}_9\text{Si}_{15-x}\text{B}_3$ .

Atom	Site	SOF	x	y	z	$U_{\text{eq}}^{[a]}$
<b><math>\text{Tb}_9\text{Si}_{15-x}\text{B}_3</math></b>						
Tb1	$9d$		0.6707(1)	0	0	0.0059(1)
Si1	$9e$	0.80(2)	0.291(2)	0	1/2	0.018(2)
Si2	$6c$		0	0	0.1704(5)	0.019(2)
B1	$3b$		0	0	1/2	0.015(3)
<b><math>\text{Yb}_9\text{Si}_{15-x}\text{B}_3</math></b>						
Yb1	$9d$		0.6711(5)	0	0	0.0095(2)
Si1	$9e$	0.87(4)	0.282(2)	0	1/2	0.025(3)
Si2	$6c$		0	0	0.1700(2)	0.020(3)
B1	$3b$		0	0	1/2	0.024(8)

<sup>[a]</sup>  $U_{\text{eq}} (\text{\AA}^2)$  is defined as one third of the trace of orthogonalized  $U_{ij}$  tensor.

**Table 3.** Anisotropic displacement parameters for  $\text{Tb}_9\text{Si}_{15-x}\text{B}_3$  and  $\text{Yb}_9\text{Si}_{15-x}\text{B}_3$ .

Atom	$U_{11}$	$U_{22}$	$U_{33}$	$U_{12}$	$U_{13}$	$U_{23}$
<b><math>\text{Tb}_9\text{Si}_{15-x}\text{B}_3</math></b>						
Tb1	0.0051(1)	0.0051(1)	0.0056(1)	0.0009(3)	-0.0001(1)	0.0001(1)
Si1	0.016(3)	0.016(3)	0.007(6)	0.0000(2)	-0.0001(7)	-0.0003(14)
Si2	0.023(3)	0.023(3)	0.010(4)	0.011(1)	0	0
B1	0.04(2)	0.04(2)	0.02(1)	0.017(12)	0	0
<b><math>\text{Yb}_9\text{Si}_{15-x}\text{B}_3</math></b>						
Yb1	0.0100(4)	0.0100(4)	0.0083(6)	0.0050(2)	-0.0013(2)	-0.00013(2)
Si1	0.034(4)	0.034(4)	0.019(2)	0.026(4)	0.0003(4)	-0.0003(4)
Si2	0.023(4)	0.023(4)	0.015(3)	0.012(2)	0	0
B1	0.04(2)	0.04(2)	0.02(1)	0.02(1)	0	0

A projection of the  $\text{Yb}_9\text{Si}_{15-x}\text{B}_3$  structure onto the crystallographic  $ab$  plane and the coordination polyhedra for all atoms are shown in Figure 1. The Yb atoms are surrounded by 12 metalloid atoms, which form a hexagonal prism and 8 additional metal atoms outside the faces of the prism (Figure 1b). Their coordination number (CN) is therefore 20. The boron and silicon atoms are situated in trigonal prisms formed by ytterbium atoms, with additional metalloid atoms outside the rectangular faces of the prisms (CN = 9, Figure 1, c and d).

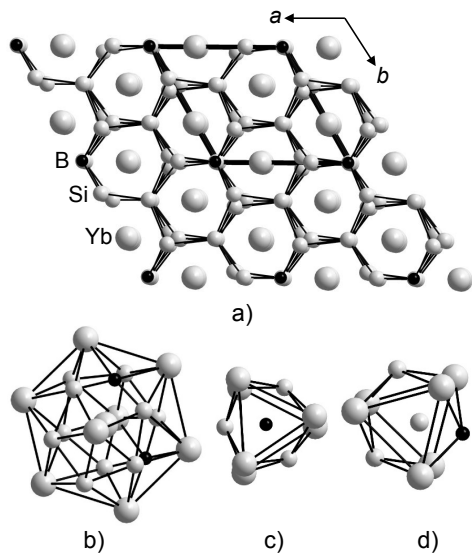


**Figure 1.** Projection of the  $\text{Yb}_9\text{Si}_{15-x}\text{B}_3$  crystal structure onto the crystallographic  $ab$  plane (a) and coordination polyhedra of the Yb (b), B (c), and Si (d) atoms.

The structure of  $\text{Yb}_9\text{Si}_{15-x}\text{B}_3$  can be considered as a ternary derivative of the  $\text{AlB}_2$  and  $\text{Th}_3\text{Pd}_5$  types of structures over a mechanism of ordering in the metalloid sublattice. The tripling of the  $c$  parameter presents a relationship to the  $\text{Yb}_3\text{Si}_5$  ( $\text{Th}_3\text{Pd}_5$  type) arrangement<sup>[7]</sup> with  $a \approx a'$  and  $c \approx 3c'$  with respect to the cell parameters of  $\text{Yb}_3\text{Si}_5$  ( $a' = 6.504$ ,  $c' = 4.092$  Å).<sup>[16]</sup> Owing to the vacancies, the silicon slab in the  $\text{Yb}_5\text{Si}_3$  structure consists of twelve-membered rings, which share common edges and extend infinitely in the  $ac$  plane. Such rings are observed also in the  $\text{RSi}_{1.7}$  structures but they only extend along the  $[001]$  direction.<sup>[13]</sup> Vacant sites in the structure of  $\text{Yb}_3\text{Si}_5$  are occupied with boron atoms in the structure of  $\text{Yb}_9\text{Si}_{15-x}\text{B}_3$ . Consequently, the presence or absence of inserted boron atoms in the new structure was the subject of a careful examination of the difference Fourier syntheses, interatomic distances and structural analysis. Insertion of boron atoms into the vacancies of the silicon slab induces a weak deformation of the  $[\text{Si}_5\text{B}]$  hexagons and some weak corrugation of the metalloid network. Figure 2 displays three layers formed by  $[\text{Si}_5\text{B}]$  hexagons of the structure  $\text{Yb}_9\text{Si}_{15-x}\text{B}_3$  along  $[001]$ . Ideal  $z$  coordinates of silicon and boron atoms are shown on the left hand-side of Figure 2b for a fully planar metalloid network. The slight deviation from planarity observed in the real structure is shown on the right-hand side of Figure 2b. Each B1 atom is bonded to three silicon atoms Si1 with distances of  $d_{\text{B1-Si1}} = 1.93(1)$  and  $1.850(11)$  Å in  $\text{Tb}_9\text{Si}_{15-x}\text{B}_3$  and  $\text{Yb}_9\text{Si}_{15-x}\text{B}_3$ , respectively. These distances are rather short, ca. 3% and 8% shorter, respectively, than those measured in  $\beta\text{-SiB}_3$ ,<sup>[18, 19]</sup>  $\text{SiB}_{30}$ ,<sup>[20]</sup>  $\text{MgB}_{12}\text{Si}_2$ ,<sup>[21]</sup> or  $\text{Li}_2\text{B}_{12}\text{Si}_2$ ,<sup>[22]</sup> for instance. Indeed, DFT optimization gives slightly longer Si-B bond distances, closer to those experimentally measured in the latter compounds (*vide supra*). With  $d_{\text{Si1-Si2}} = 2.378(9)$  in  $\text{Tb}_9\text{Si}_{15-x}\text{B}_3$  and  $2.384(12)$  Å in  $\text{Yb}_9\text{Si}_{15-x}\text{B}_3$ , Si-Si distances are close to the sum of the covalent radius of silicon ( $r_{\text{Si}} = 1.17$  Å). Tb-Tb distances of  $3.803(1)$  and  $4.135(1)$  Å and Yb-Yb distances of  $3.748(1)$  and  $3.824(1)$  Å are measured.  $R$ -Si and  $R$ -B distances

are close to the average distances generally encountered in corresponding binary rare-earth metal borides and silicides. The alternate stacking of the  $[\text{Si}_5\text{B}]$  hexagons above and below the  $R$  layer leads to many different  $R$ -Si and  $R$ -B distances (Table 4).

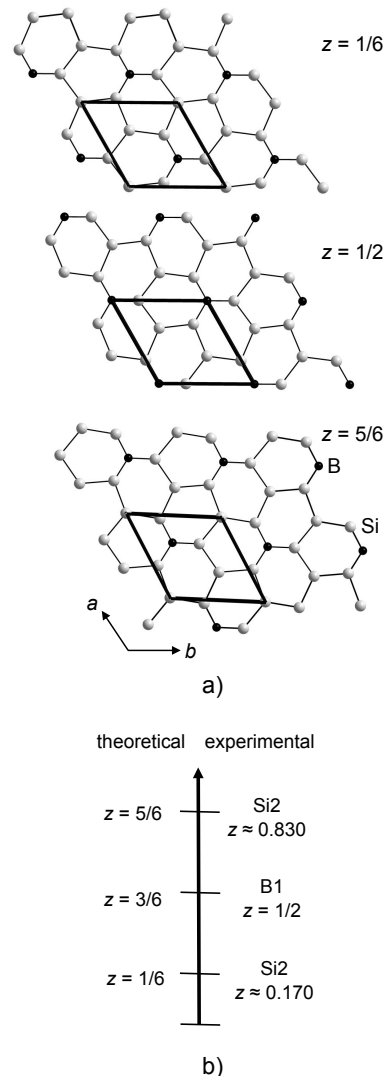


**Figure 2.** Projection of the three different layers of the  $\text{Yb}_9\text{Si}_{15-x}\text{B}_3$  structure (a) and the sequence of the boron and silicon atoms in the different layer (b) along  $[001]$ .

**Table 4.** Selected interatomic distances ( $d$ , Å) for  $\text{Tb}_9\text{Si}_{15-x}\text{B}_3$  and  $\text{Yb}_9\text{Si}_{15-x}\text{B}_3$ .

Atom	$d$	Atom	$d$	Atom	$d$
<b><math>\text{Tb}_9\text{Si}_{15-x}\text{B}_3</math></b>					
Tb1-2Si1	2.936(4)	Si1-2Tb1	2.936(4)	Si2-3Tb1	3.015(4)
2Si1	2.962(4)	2Tb1	3.237(1)	3Tb1	3.048(5)
2Si1	3.239(1)	2Tb1	2.962(4)	3Si1	2.378(9)
2Si2	3.015(4)	2Si2	2.378(9)		
2Si2	3.048(5)	2B1	1.93(1)	B1-6Yb1	3.045(1)
2B1	3.045(1)			3Si1	1.93(1)
<b><math>\text{Yb}_9\text{Si}_{15-x}\text{B}_3</math></b>					
Yb1-2Si1	2.882(12)	Si1-2Yb1	2.882(12)	Si2-3Yb1	3.004(12)
2Si1	2.911(5)	2Yb1	3.2446(7)	3Yb1	2.981(17)
2Si1	3.25(1)	2Yb1	2.911(12)	3Si1	2.384(12)
2Si2	3.004(2)	2Si2	2.384(2)		
2Si2	2.981(2)	2B1	1.850(11)	B1-6Yb1	3.047(1)

2B1 3.047(1) 3Si1 1.850(11)

The structural relationship between the crystal structures of the hettotype  $\text{YbSi}_{15-x}\text{B}_3$  and the aristotype  $\text{AlB}_2$  can be derived from a Bärnighausen tree.<sup>[23, 24]</sup> The corresponding group-subgroup scheme is shown in Figure 3. The symmetry reductions from  $\text{AlB}_2$  to  $\text{YbSi}_{15-x}\text{B}_3$  structure may be subdivided into three steps. A *translationsgleiche* transition of index 2 leads to the simplest ternary  $\text{SrPtSb}$  structure of space group  $P\bar{6}m2$ , an ordered variant of the  $\text{AlB}_2$  structure type.<sup>[25]</sup> Here (Figure 3), each planar hexagon is built up from three platinum and three antimony atoms in an ordered manner. The following *translationsgleiche* step lowers the symmetry to the trigonal space group  $P312$  (Nr. 149). The last and most important step is again a *klassengleiche* transition of order 3, corresponding to the transformation  $a-b$ ,  $a+2b$ ,  $3c$ . Lowering the symmetry to the trigonal system  $R32$  (Nr. 155) leads to a splitting of the  $1f$  site into a six-fold  $6c$  site (0, 0, 0.17) and a threefold  $3b$  site (0, 0, 1/2) occupied by silicon and boron atoms, respectively. The different nature of the non-metal atoms forming the hexagons in the structure leads to the puckering of the initial planar metalloid net. From another hand, the simple filling by boron atoms of the vacancies in the silicon slab of the  $\text{Yb}_3\text{Si}_5$  structure,<sup>[16]</sup> cannot be simply reduced from the group-subgroup relation over the  $\text{Th}_3\text{Pd}_5$  structure.

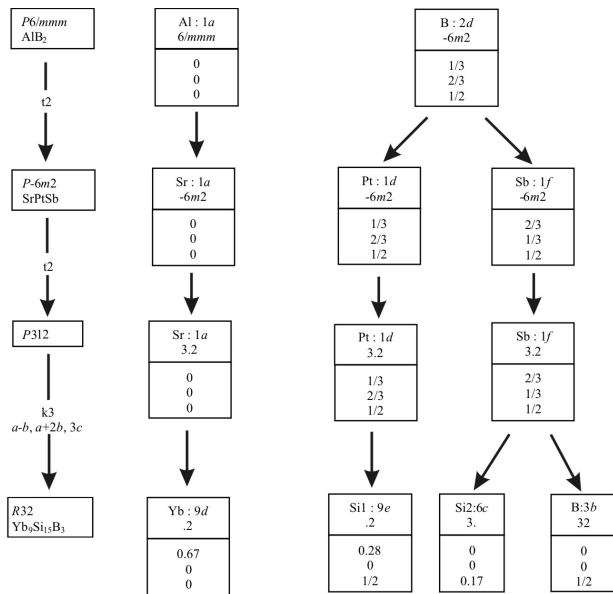


**Figure 3.** Group-subgroup scheme in the Bärnighausen formalism for the structures  $\text{AlB}_2$ ,  $\text{SrPtSb}$ , and  $R_9\text{Si}_{15-x}\text{B}_3$ . The indices for the *translationsgleiche* ( $t$ ) symmetry reductions, the unit cell transformations, and the evolution of the atomic parameters are given.

Assuming in a first approximation full occupation of Si1 in 9e position and a simple Zintl–Klemm ionic bonding scheme<sup>[25]</sup> between the metal and the non-metal atoms, anionic

silicon atoms and dianionic boron atoms can be considered resulting in the ionic formulation  $[\text{R}_9]^{21+}[\text{Si}]_{15}[\text{B}^{2-}]_3$ . If we assume such a charge distribution, some electrons must remain available for metal–metal bonding in the compounds  $R_9\text{Si}_{15-x}\text{B}_3$ . Indeed, negative charges attributed to the three-connected  $sp^2$  Si and B atoms come from the fact that only single Si–Si or Si–B bonds are observed in the Si/B network. Therefore, it is assumed that they obey the octet rule although they violate the hybridization rule.

Periodic density functional theory (DFT) calculations were carried out in order to gain insight on their structural and electronic properties (see the Experimental section for computational details). Full occupation of Si1 in 9e position (see above) was considered to reduce the computational effort, i.e., computations were performed on  $R_9\text{Si}_{15}\text{B}_3$  model structures and on the related binary compound  $\text{Yb}_3\text{Si}_5$ <sup>[16]</sup> for comparison.

Optimized unit cell parameters and interatomic distances are given and compared to the experimental ones in Table 5. The computed values quite satisfactorily mimic those of the crystallographically characterized compounds. Especially, the M–M bond lengths are well reproduced and are consistent with the lanthanide contraction law experimentally ascertained. Overall, as often computed for crystal structures relaxed using LDA or GGA functionals, a slight overestimation of all metrical parameters (ca. 1 %) is noted.

**Table 5.** Selected optimized interatomic distances and cell parameters (Å) for  $\text{Yb}_3\text{Si}_5$  and “ $R_9\text{Si}_{15}\text{B}_3$ ” ( $R = \text{Yb}, \text{Tb}$ ) compounds. Experimental values are given in brackets.

	$\text{Yb}_3\text{Si}_5$	“ $\text{Yb}_9\text{Si}_{15}\text{B}_3$ ”	“ $\text{Tb}_9\text{Si}_{15}\text{B}_3$ ”
<i>a</i>	6.5348 (6.5049)	6.5909 (6.5896)	6.6961 (6.6681)
<i>c</i>	4.1295 (4.0923)	12.2946 (12.2599)	12.5009 (12.4040)
<i>R–R</i>	3.704 (3.632)	3.824 (3.748) 3.857 (3.825)	3.861 (3.809) 3.869 (3.871)
<i>R–Si1</i>	3.007 (3.006) 3.180 (3.261)	2.939 (2.882) 2.938 (2.911) 3.213 (3.250)	2.984 (2.936) 2.988 (2.962) 3.204 (3.239)
<i>R–Si2</i>	2.938 (2.929) 2.958 (2.930)	3.046 (2.981) 3.067 (3.004)	3.051 (3.015) 3.054 (3.048)
<i>R–B1</i>		3.065 (3.008)	3.055 (3.045)
Si1–Si1	3.094 (3.033)		
Si1–Si2	2.453 (2.404)	2.340 (2.384)	2.340 (2.379)
B–Si1		2.025 (1.850)	2.029 (1.930)

The total and atom-projected density of states (DOS) for  $\text{Yb}_3\text{Si}_5$ ,  $\text{Yb}_9\text{Si}_{15}\text{B}_3$ , and  $\text{Tb}_9\text{Si}_{15}\text{B}_3$  were computed (see Figure 4 and Figure S1). Except the position of the Fermi level  $\epsilon_F$  in the sharp peak deriving from the  $f$  orbitals, comparable results are observed for  $\text{Yb}_9\text{Si}_{15}\text{B}_3$  and  $\text{Tb}_9\text{Si}_{15}\text{B}_3$  (compare Figures 4b and S1). Consequently, only the results obtained for the former are commented here. A comparison of the total and atom-projected

DOS of the binary phase  $\text{Yb}_3\text{Si}_5$  and the ternary phase  $\text{Yb}_9\text{Si}_{15}\text{B}_3$  (Figure 4) indicates more dispersed DOS, especially below  $\epsilon_F$  in the energy window  $[-5; -2.5]$  eV for the former. Nevertheless, in both cases, metallic conductivity is expected with  $\epsilon_F$  lying in a pronounced peak of DOS made from all the constituting elements, reflecting substantial metal–nonmetal covalent interaction. Interestingly, no holes in the DOS are observed close to  $\epsilon_F$  which could favor specific electron counts and therefore specific stoichiometries. On the other hand, some homogeneity range might be possible, reflected by the refined occupancy factors of Si1, which differ in  $\text{Yb}_9\text{Si}_{15-x}\text{B}_3$  and  $\text{Tb}_9\text{Si}_{15-x}\text{B}_3$ , (see Table 2). We will come back to this point later.

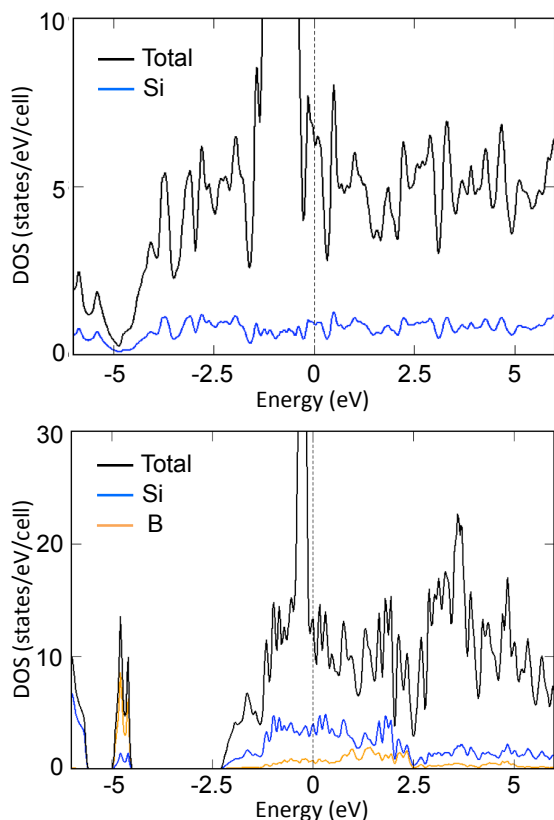


**Figure 4.** Total and atom-projected DOS for  $\text{Yb}_3\text{Si}_5$  (top) and  $\text{Yb}_9\text{Si}_{15}\text{B}_3$  (bottom).  $\epsilon_F$  set at 0 eV.

Covalent character between the metal and the non-metal atoms is confirmed by the analysis of crystal orbital Hamiltonian population (COHP) curves which indicate energetic contributions of crystal orbitals between atoms.<sup>[26]</sup> Those computed for the Yb-Si1, Yb-Si2, Yb-B1, Yb-Yb, Si1-Si2, and Si1-B1 contacts in the  $\text{Yb}_9\text{Si}_{15}\text{B}_3$  structure are sketched in Figure 5. Their inspection shows that the bonding between metal and non-metal atoms is nearly maximized in this compound, except that between the atoms Si1 and B1, the COHP curve of which shows some antibonding states below  $\epsilon_F$ . This is an important result. Although the value of the corresponding integrated COHP is a rather high (ICOHP = -0.402 Ry/cell), fractional occupancy of Si1 should

shift down the Fermi level – a rigid band model is assumed – and diminish the number of occupied Si1-B1 antibonding states. This is probably why full occupancy of Si1 is not observed in  $\text{Yb}_9\text{Si}_{15-x}\text{B}_3$  ( $x = 1.17$ ) and  $\text{Tb}_9\text{Si}_{15-x}\text{B}_3$  ( $x = 1.80$ ). It is noteworthy that the Yb-Yb and Si1-Si2 COHP curves compare very well with the corresponding ones in the binary  $\text{Yb}_3\text{Si}_5$  compound (Figure S2).

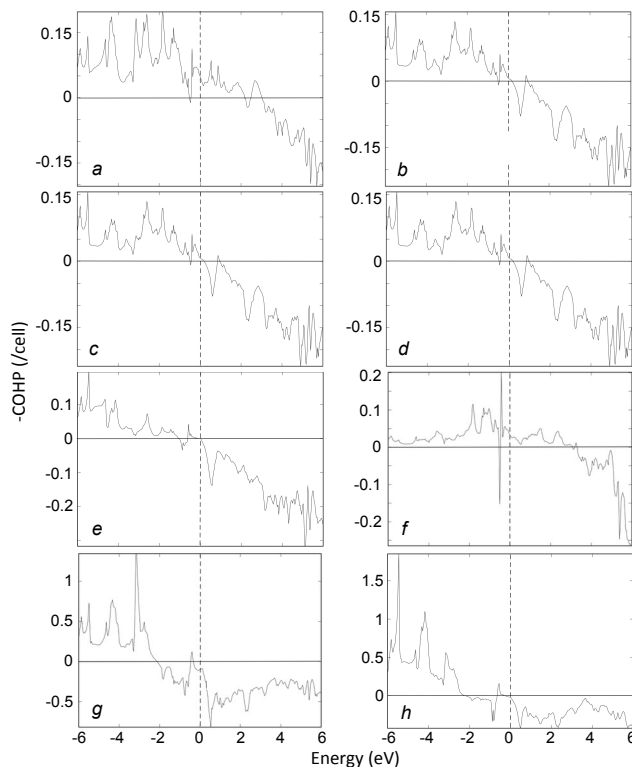


**Figure 5.** COHP curves for Yb-Si1 = 2.938 and 3.213 Å (a, b), Yb-Si2 = 3.046 and 3.067 Å (c, d), Yb-B1 = 3.065 Å (e), Yb-Yb = 3.824 Å (f), Si1-Si2 = 2.340 Å (g), and Si1-B1 = 2.025 Å (h) contacts in  $\text{Yb}_9\text{Si}_{15}\text{B}_3$ .  $\epsilon_F$  set at 0 eV.

As expected, strong covalent interactions occur between the non-metals atoms. This is supported by the large ICOHP values computed for both Si1-Si2 and Si1-B1 (-0.191 and -0.402 Ry/cell, respectively). Although a strict comparison cannot be made, the value of the former is of the same order than the Si1-Si2 ICOHP value computed for the binary  $\text{Yb}_3\text{Si}_5$  (-0.175 Ry/cell). ICOHP values for Yb-Si (-0.032 and -0.057 Ry/cell for Yb-Si1 and -0.054 and -0.056 Ry/cell for Yb-Si2) and Yb-B1 (-0.031 Ry/cell) contacts are of the same order of magnitude and reflects substantial metal-non-metal interactions. These interactions are also supported by the atomic net charges computed for  $\text{Yb}_9\text{Si}_{15}\text{B}_3$  ( $[\text{Yb}^{0.56+}]_3$ ,  $[\text{Si1}^{0.14}]_9$ ,  $[\text{Si2}^{0.13}]_6$ ,  $[\text{B1}^{1.00-}]_3$ ), which indicate some electron transfer from the metal to the non-metal atoms somewhat in agreement with the Zintl-Klemm ionic formulation proposed above. Slightly weaker charge transfer is computed in the binary  $\text{Yb}_3\text{Si}_5$  ( $[\text{Yb}^{0.32+}]_3$ ,  $[\text{Si1}^{0.15-}]_3$ ,  $[\text{Si2}^{0.26-}]_2$ ).

## Conclusions

Two novel ternary borosilicides of formula  $R_9\text{Si}_{15-x}\text{B}_3$  were prepared with  $R = \text{Tb}, \text{Yb}$  using tin flux method. Their crystal structure was solved from single-crystal X-ray diffraction data, indicating a new structure type, which can be derived from the structure of the binary silicide  $\text{Yb}_3\text{Si}_5$  (nonstoichiometric  $\text{AlB}_2$  type) with partial occupancy of Si atoms and filling of the vacant site. The silicon and boron atoms form a two-dimensional planar network made of  $[\text{Si}_5\text{B}]$  hexagons. Theoretical calculations show substantial covalent interactions between the metal and nonmetal elements. The small percentage of silicon atoms, which are missing in these nonstoichiometric compounds, probably allows strengthening boron-metal and boron-silicon bonding.

## Experimental Section

**Synthesis and analysis:** Single crystals of the title compound were obtained using tin as a metal flux. First, suitable amounts of silicon (purity 99.999%) and boron (99.99%) as powders and rare-earth metals (99.9%) as chips, in the nominal atomic ratio  $R/\text{Si}/\text{B} = 3/1/2$  ( $R = \text{Tb}, \text{Yb}$ ), were mixed together and cold-pressed into pellets (each sample of about 1 g). A large excess of tin as granules was then added in order to obtain a tin content of about 80% in weight. Then, the mixtures were sealed in silica tubes under vacuum and annealed at 1173 K during 5 days. After quenching in air, the molten buttons were slowly dissolved in diluted hydrochloric acid. The yield of the title materials from a synthesis batch is about 60%, according X-ray powder data and only  $\text{REB}_4$  is detected as byproduct. Then, shiny grey truncated platelet-like single crystals were extracted for structure determination. Electron probe microanalyses on single crystals, using energy-dispersive spectroscopy (EDS) with the help of a scanning electron microscope (Jeol JSM-6400), confirmed terbium, ytterbium and silicon being present in nominal overall content (in at.%):  $R/\text{Si} = 40.1/59.9$  (standard deviations estimated less than 1 at.%). Unfortunately, no boron content could be determined by disposable quantitative microanalysis.

**X-ray diffraction and structure refinement:** The structure determination was performed on single crystals. Platelet-like metallic luster single crystals non-reactive to air were obtained for all samples. First, single crystals were studied by conventional X-ray photographic methods (oscillating crystal and Weissenberg). Second, X-ray intensity data collection of  $\text{Yb}_9\text{Si}_{15}\text{B}_3$  was performed from a hemisphere of 197 images in a total exposure time of 144 min on a four-circle Nonius Kappa diffractometer, equipped with a CCD area detector employing graphite-monochromatized  $\text{Mo K}\alpha$  radiation ( $\lambda = 0.71073 \text{ \AA}$ ). The orientation matrix and the unit cell were derived from the first 10 data frames using the program DENZO.<sup>[27]</sup> Absorption correction was applied with the help of the program NUMABS<sup>[28]</sup> with  $T_{\text{min}} = 0.008$  and  $T_{\text{max}} = 0.054$ . Single crystal diffraction data of  $\text{Tb}_9\text{Si}_{15}\text{B}_3$  was collected at room temperature on a STOE IPDS II image plate diffractometer with monochromatized  $\text{MoK}\alpha$  radiation. X-ray intensity data collection of  $\text{Tb}_9\text{Si}_{15}\text{B}_3$  was performed from a hemisphere of 180 images in a total exposure time of 360 min. Crystal structures of  $\text{Yb}_9\text{Si}_{15}\text{B}_3$  and  $\text{Tb}_9\text{Si}_{15}\text{B}_3$  were solved by direct methods (SIR97),<sup>[29]</sup> and least-squares refinements and difference Fourier syntheses were run with the beta version of the JANA2000 software<sup>[30]</sup> (full matrix least-squares on  $F$ ) and the program SHELX-97<sup>[31]</sup> within the WinGX program package<sup>[32]</sup> (full matrix least-squares on  $F^2$ ) with anisotropic atomic displacement parameters for all atoms. The refinements converged well, and the light atoms could be located from

the difference Fourier maps. Crystal structure and refinement details are given in Table 1. The atomic coordinates and displacement parameters are listed in Table 2, selected interatomic distances and bond angles are summarized in Table 3. The drawings were prepared with the program DIAMOND.<sup>[33]</sup>

**Computational procedures:** Geometry optimizations of  $\text{Yb}_3\text{Si}_5$ ,  $\text{Yb}_9\text{Si}_{15}\text{B}_3$  and  $\text{Tb}_9\text{Si}_{15}\text{B}_3$  were carried out using density functional theory (DFT) using the Perdew-Burke-Ernzerhof (PBE) functional<sup>[34]</sup> implemented in the CASTEP16.1 code.<sup>[35]</sup> The structures were fully optimized (lattice vectors and atomic positions) and the maximum gradient threshold was set to 0.05 eV/Å. All ultra-soft pseudopotentials were generated using the OTF ultrasoft pseudopotential generator included in the program. Relativistic effects were taken into account for all elements by using scalar relativistic pseudo-potentials. The cut-off energy for plane-waves was set at 500 eV. The electronic wave function was sampled with 110  $k$ -points in the first Brillouin zone using the Monkhorst-Pack method.<sup>[36]</sup>

Density of states (DOS) were obtained using the full-potential linearized augmented plane wave (FLAPW) approach as implemented in the WIEN2K code<sup>[37]</sup> in the GGA-DFT approximation with spin-orbit coupling. The PBE<sup>[34]</sup> functional was used for the exchange correlation energy functional. A plane wave cut-off corresponding to  $R_{\text{MT}}K_{\text{max}} = 7$  was used. The charge density was Fourier expanded up to  $G_{\text{max}} = 16 \text{ \AA}^{-1}$ . Total energy convergence was achieved with a Brillouin zone (BZ) integration mesh of 500  $k$ -points and the density of states was shifted in order that the Fermi level lies at 0 eV.

Finally, crystal orbital Hamiltonian population (COHP) and integrated COHP (ICOHP) were obtained with the scalar relativistic tight-binding linear muffin-tin orbital method (LMTO) in the atomic sphere approximation including the combined correction obtained with TB-LMTO-ASA code<sup>[38]</sup> for the  $\text{Yb}_9\text{Si}_{15}\text{B}_3$  compound. Exchange-correlation was treated with LDA using the von Barth-Hedin local exchange-correlation potential.<sup>[39]</sup> Within the LMTO formalism, interatomic space is filled with interstitial spheres. The optimal positions and radii of these additional empty spheres are determined by the procedure described by von Barth *et al.*<sup>[40]</sup> Six nonsymmetry-related empty spheres were introduced in these calculations. The eigenvalue problem was solved using a minimal basis set obtained from the Löwdin downfolding technique removing all empty spheres functions from the calculations. The  $k$ -space integration was performed using the tetrahedron method.<sup>[41]</sup> Charge self-consistency and average properties were obtained from 96 irreducible  $k$ -points. As recommended, a reduced basis set (in which empty sphere LMTOs were down-folded) was used the COHP calculations. COHP curves were shifted so that the Fermi level lies at 0 eV.

**Supporting Information** (see footnote on the first page of this article): DOS curve for  $\text{Tb}_9\text{Si}_{15}\text{B}_3$  and COHP curves for  $\text{Yb}_3\text{Si}_5$  can be found in the supporting information.

## Acknowledgements

The authors thank W. Hölle (MPI FKF, Stuttgart) for X-ray intensity data collection.

**Keywords:** borosilicide • crystal structure • density functional calculations • electronic structure • rare-earth metal borosilicide

## References

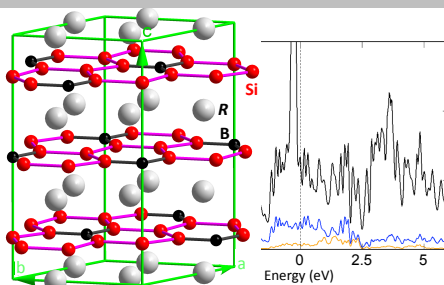
- [1] T. Mori, Higher borides. In *Handbook on the Physics and Chemistry of Rare Earths* (Eds: K. A. Gschneidner Jr., J.-C. Bunzli and V. Pecharsky), North-Holland, Amsterdam 2008. Vol. 38. P. 105–173.
- [2] J. Roger, V. Babizhetskyy, T. Guizouarn, K. Hiebl, J.-F. Halet, R. Guérin, The ternary RE-Si-B systems (RE = Dy, Ho, Er and Y) at 1270 K: Solid state equilibria and magnetic properties of the solid solution  $REB_{2-x}Si_x$  (RE = Dy and Ho). *J. Alloys Compd.* **2006**, *417*, 72–84.
- [3] J. Roger, V. Babizhetskyy, K. Hiebl, J.-F. Halet, R. Guérin, Solid state phase equilibria in the ternary Nd-Si-B system at 1270 K. *J. Alloys Compd.* **2006**, *415*, 73–84.
- [4] V. Babizhetskyy, J. Roger, J. Bauer, S. Députier, R. Jardin, R. Guérin, Solid State Phase Equilibria in the Gd-Si-B System at 1270 K. *J. Solid State Chem.* **2004**, *177*, 415–424.
- [5] V. Babizhetskyy, J. Roger, S. Deputier, R. Guérin, R. Jardin, J. Bauer, K. Hiebl, C. Jardin, J.-Y. Saillard, J.-F. Halet, Synthesis, crystal structure, physical properties and chemical bonding of  $Gd_5Si_2B_8$ : An unprecedented example of a ternary rare earth metal silicide boride compound. *Angew. Chem. Int. Ed.* **2004**, *43*, 1979–1983.
- [6] J. Roger, V. Babizhetskyy, S. Cordier, J. Bauer, K. Hiebl, L. Le Pollès, S. E. Ashbrook, J.-F. Halet, R. Guérin, Crystal structures, physical properties and NMR experiments on the ternary rare-earth metal silicide boride compounds  $RE_5Si_2B_8$  (RE = Y, Sm, Gd, Tb, Dy, Ho). *J. Solid State Chem.* **2005**, *178*, 1851–1863.
- [7] J. Roger, M. Ben Yahia, V. Babizhetskyy, J. Bauer, S. Cordier, R. Guérin, K. Hiebl, X. Rocquefelte, J.-Y. Saillard, J.-F. Halet,  $Mn_5Si_3$ -type host-interstitial boron rare-earth metal silicide compounds  $RE_5Si_3$ : Crystal structures, physical properties and theoretical considerations. *J. Solid State Chem.* **2006**, *179*, 2310–2328.
- [8] R. Jardin, V. Babizhetskyy, R. Guérin, J. Bauer, Crystal structure of the rare earth borosilicide  $Er_8Si_{17}B_3$ . *J. Alloys Compd.* **2003**, *353*, 233–239.
- [9] Yu. B. Kuz'ma, N. F. Chaban, Binary and Ternary Systems Containing Boron, Metallurgiya, Moscow, 1990 (in Russian).
- [10] N. F. Chaban, Yu. B. Kuz'ma, Phase equilibria in Er-Si-B. *Inorg. Mater.* **2000**, *36*, 1057–1058.
- [11] N. F. Chaban, Yu. B. Kuz'ma, X-ray investigation of ternary system {Y, La, Ce}-{Al, Si}-B. *Dopov. AN. URSR.* **1971**, *11*, 1048–1050 (in Ukrainian).
- [12] M. G. Kanatzidis, R. Pöttgen, W. Jeitschko, The metal flux: a preparative tool for the exploration of intermetallic compounds. *Angew. Chem., Int. Ed.* **2005**, *44*, 6996–7023.
- [13] J. Roger, V. Babizhetskyy, R. Jardin, R. Guérin, C. Moinet, U. Burkhardt, J.-F. Halet, Tin flux synthesis of rare-earth metal silicide compounds  $RESi_{1.7}$  (RE = Dy, Ho): A novel ordered structure derived from the  $AlB_2$  type. *Z. Kristallogr.* **2006**, *221*, 502–510.
- [14] W. Hofmann, W. Jäniche, Der Strukturtyp von Aluminiumborid ( $AlB_2$ ). *Naturwissenschaften*, **1935**, *50*, 851.
- [15] J. R. Thomson, The crystal structure of  $Th_3Pd_5$  and  $Th_3Pt_5$ . *Acta Crystallogr.* **1963**, *16*, 320–321.
- [16] R. Pöttgen, R.-D. Hoffmann, D. Kussmann, The binary silicides  $Eu_5Si_3$  and  $Yb_5Si_3$  – synthesis, crystal structure, and chemical bonding. *Z. Anorg. Allgem. Chem.* **1998**, *624*, 945–951.
- [17] A. Grytsiv, D. Kaczorowski, A. Leithe-Jasper, V. H. Tran, A. Pikul, P. Rogl, M. Potel, H. Noël, M. Bohn, T. Velikanova, On the System Silicon-Ytterbium: Constitution, Crystal Chemistry, and Physical Properties. *J. Solid State Chem.* **2002**, *163*, 178–185.
- [18] J. R. Salvador, D. Bilc, S. D. Mahanti, M. G. Kanatzidis, Stabilization of  $\beta$ - $SiB_3$  from Liquid Ga: A Boron-Rich Binary Semiconductor Resistant to High-Temperature Air Oxidation. *Angew. Chem., Int. Ed.* **2003**, *42*, 1929–1932.
- [19] D. Eklöf, A. Fischer, A. Ektarawong, A. Jaworski, A. J. Pell, J. Grins, S. I. Simak, B. Alling, Y. Wu, M. Widom, W. Scherer, U. Häussermann, Mysterious  $SiB_3$ : Identifying the Relation between  $\alpha$ - and  $\beta$ - $SiB_3$ . *ACS Omega* **2019**, *4*, 18741–18759.
- [20] J. Roger, V. Babizhetskyy, J.-F. Halet, R. Guérin, Boron–silicon solid solution: synthesis and crystal structure of a carbon-doped boron-rich  $SiB_n$  ( $n=30$ ) compound. *J. Solid State Chem.* **2004**, *177*, 4167–4174.
- [21] T. Ludwig, H. Hillebrecht, Synthesis and crystal structure of  $MgB_{12}Si_2$ —The first ternary compound in the system B/Mg/Si. *J. Solid State Chem.* **2006**, *179*, 1623–1629.
- [22] N. Vojteer, M. Schroeder, C. Röhr, H. Hillebrecht,  $Li_2B_{12}Si_2$ : The First Ternary Compound in the System Li/B/Si: Synthesis, Crystal Structure, Hardness, Spectroscopic Investigations, and Electronic Structure. *Chem. - Eur. J.* **2008**, *14*, 7331–7342.
- [23] H. Bärnighausen, Group-subgroup relations between space groups: a useful tool in crystal chemistry. *Commun. Math. Chem.* **1980**, *9*, 139–175.
- [24] R.-D. Hoffmann, R. Pöttgen R.,  $AlB_2$ -related intermetallic compounds – a comprehensive view based on group-subgroup relations. *Z. Kristallogr.* **2001**, *216*, 127–145.
- [25] G. Wenski, A. Mewis, Trigonal-planar koordiniertes Platin: Darstellung und Struktur von  $SrPtAs$  (Sb),  $BaPtP$  (As, Sb),  $SrPt_xP_{2-x}$ ,  $SrPt_xAs_{0.9}$  und  $BaPt_xAs_{0.8}$ . *Z. Anorg. Allg. Chem.* **1986**, *535*, 100–122.
- [26] (a) E. Zintl, Intermetallische Verbindungen. *Angew. Chem.* **1939**, *52*, 1; (b) W. Klemm, Metalloids and their compounds with the alkali metals. *Proc. Chem. Soc. (London)* **1958**, 329–364.
- [27] R. Dronskowski, P. E. Blöchl, Crystal Orbital Hamilton Populations (COHP): Energy-resolved Visualization of Chemical Bonding in Solids Based on Density-Functional Calculations. *J. Phys. Chem.* **1993**, *97*, 8617–8624.
- [28] Nonius Kappa CCD Program Package COLLECT, DENZO, SCALEPACK, Nonius BV, Delft, The Netherlands, 1998.
- [29] P. Coppens, in *Crystallographic Computing*, (Eds.: F.R. Ahmed, S.R. Hall, C.P. Huber) Munksgaard, Copenhagen, 1970, pp. 250–270.
- [30] A. Altomare, M. C. Burla, M. Camalli, B. Carrozzini, G. L. Casciarano, C. Giacovazzo, A. Guagliardi, A. G. G. Moliterni, G. Polidori, R. Rizzi, SIR97: A new tool for crystal structure determination and refinement. *J. Appl. Crystallogr.* **1999**, *32*, 115–119.
- [31] V. Petricek, M. Dusek, JANA2000, Program for Crystal Structure Refinement, Institute of Physics, Academy of Sciences of the Czech Republic, Praha.
- [32] G. M. Sheldrick, SHELXL-97, Program for the Refinement of Crystal Structures. University of Göttingen, Germany 1997.
- [33] L. J. Farrugia, WinGX (Version 1.64.05), *J. Appl. Crystallogr.* **1999**, *32*, 837–838.
- [28] K. Brandenburg, Diamond (version 2.1c), Crystal and Molecular Structure Visualization, Crystal Impact - H. Putz & K. Brandenburg GbR, Bonn (Germany) 1999.
- [34] J. P. Perdew, K. Burke, M. Ernzerhof, Generalized Gradient Approximation Made Simple. *Phys. Rev. Lett.*, **1996**, *77*, 3865–3868.
- [35] S. J. Clark, M. D. Segall, C. J. Pickard, P. J. Hasnip, M. J. Probert, K. Refson, M. C. Payne, First principles methods using CASTEP. *Z. Kristallogr.* **2009**, *220*, 567–570.
- [36] H. J. Monkhorst, J. D. Pack, Special Points for Brillouin-Zone Integrations. *Phys. Rev. B* **1976**, *13*, 5188–5192.
- [37] a) K. Schwarz, P. Blaha, G. K. H. Madsen, Electronic structure calculations of solids using the WIEN2k package for material sciences. *Comp. Phys. Comm.* **2002**, *147*, 71–76. b) P. Blaha, K. Schwarz, G. K. H. Madsen, D. Kvasnicka, J. Luitz, WIEN2K, An Augmented Plane Wave + Local Orbitals Program for Calculating Crystal Properties. Tech. Univ. Wien, Austria, 2001.
- [38] (a) O. K. Andersen, Linear methods in band theory. *Phys. Rev. B* **1975**, *12*, 3060–3083. (b) O. K. Andersen, New methods for the one electron problem. *Europhys. News* **1981**, *12*, 4–8. (c) O. K. Andersen, O. Jepsen, Explicit, First-Principles Tight-Binding Theory. *Phys. Rev. Lett.* **1984**, *53*, 2571–2574. (d) O. K. Andersen, O. Jepsen, M. Sob,



- Electronic Band Structure and its Applications (Ed.: M. Yussouff) Springer, Berlin, Germany, 1987; pp 1–57.
- [39] H. L. Skriver, The LMTO Method; Springer, Berlin, Germany, 1984.
- [40] U. von Barth, L. Hedin, A local exchange-correlation potential for the spin polarized case. *J. Phys. C: Solid State Phys.* **1972**, *5*, 1629–1642.
- [41] O. Jepsen, O. K. Andersen, Calculated electronic structure of the sandwich d<sup>1</sup> metals LaI<sub>2</sub> and CeI<sub>2</sub>: Application of new LMTO techniques. *Z. Phys. B: Condens. Matter* **1995**, *97*, 35–47.

**Entry for the Table of Contents** (Please choose one layout)Layout 1: V. Babizhetskyy et al., Rare-earth metal borosilicides  $R_9\text{Si}_{15-x}\text{B}_3$  ( $R = \text{Tb}, \text{Yb}$ )**FULL PAPER**

Two novel ternary borosilicides  $R_9\text{Si}_{15-x}\text{B}_3$  ( $R = \text{Tb}, \text{Yb}$ ) have been synthesized from the initial elements using tin flux method.



*Volodymyr Babizhetskyy,\*  
Volodymyr Levytskyy, Régis Jardin,  
Josef Bauer, Roland Guérin, Régis  
Gautier,\* Bruno Fontaine,\* and Jean-  
François Halet\**

**Page No. – Page No.**

**Rare-earth metal borosilicides  
 $R_9\text{Si}_{15-x}\text{B}_3$  ( $R = \text{Tb}, \text{Yb}$ ): New  
ordered structures derived from  
the  $\text{AlB}_2$  structure type**

Additional Author information for the electronic version of the article.

Author: Volodymyr Babizhetskyy	ORCID identifier: 0000-0002-0267-0206
Author: Volodymyr Levytskyy	ORCID identifier: 0000-0003-0874-8833
Author: Régis Gautier	ORCID identifier: 0000-0002-8104-4982
Author: Jean-François Halet	ORCID identifier: 0000-0002-2315-4200